

Lawrence Berkeley National Laboratory

Recent Work

Title

TRANSIENT RESPONSE OF Ge:Be AND Ge:Zn FAR-INFRARED PHOTOCONDUCTORS UNDER LOW BACKGROUND PHOTON FLUX CONDITIONS

Permalink

<https://escholarship.org/uc/item/39f9g2gs>

Authors

Haegel, N.M.
Haller, E.E.

Publication Date

1986



Lawrence Berkeley Laboratory

UNIVERSITY OF CALIFORNIA

RECEIVED

LAWRENCE
BERKELEY LABORATORY

APR 7 1986

LIBRARY AND
DOCUMENTS SECTION

Engineering Division

Submitted Infrared Physics

TRANSIENT RESPONSE OF Ge:Be AND Ge:Zn
FAR-INFRARED PHOTOCONDUCTORS UNDER
LOW BACKGROUND PHOTON FLUX CONDITIONS

N.M. Haegel and E.E. Haller

January 1986

TWO-WEEK LOAN COPY

*This is a Library Circulating Copy
which may be borrowed for two weeks.*



LBL-21009
c.2

DISCLAIMER

This document was prepared as an account of work sponsored by the United States Government. While this document is believed to contain correct information, neither the United States Government nor any agency thereof, nor the Regents of the University of California, nor any of their employees, makes any warranty, express or implied, or assumes any legal responsibility for the accuracy, completeness, or usefulness of any information, apparatus, product, or process disclosed, or represents that its use would not infringe privately owned rights. Reference herein to any specific commercial product, process, or service by its trade name, trademark, manufacturer, or otherwise, does not necessarily constitute or imply its endorsement, recommendation, or favoring by the United States Government or any agency thereof, or the Regents of the University of California. The views and opinions of authors expressed herein do not necessarily state or reflect those of the United States Government or any agency thereof or the Regents of the University of California.

Transient Response of Ge:Be and Ge:Zn Far-Infrared Photoconductors
Under Low Background Photon Flux Conditions

N. M. Haegel* and E. E. Haller
Lawrence Berkeley Laboratory and
University of California
Berkeley, CA 94720

ABSTRACT

An experimental study of transient behavior of Ge:Be and Ge:Zn photoconductors to changes in photon flux rates has been performed under the low background flux conditions ($\dot{p} \approx 10^8$ photons/second) typical of astronomy and astrophysics applications. A characteristic transient behavior with time constants ranging from 0.1 to greater than 5 seconds has been observed in both materials. The detector response consists of both a fast and a slow component. The amplitude of the slow component can be up to ten times greater than the initial fast component. It has been established that this phenomena cannot be explained by current models of carrier sweep-out or dielectric relaxation. The transient behavior has been characterized as a function of temperature, electric field, photoconductive gain, and material parameters.

*Current address: Siemens AG, Erlangen, Federal Republic of Germany

INTRODUCTION

The study of the transient response of extrinsic photoconductors to changes in photon flux has traditionally been the most challenging issue in the field of infrared detector characterization. Under conditions of very low photon fluxes, where carrier densities can be as low as 10 cm^{-3} , extrinsic photoconductors are well known for exhibiting transient behavior characterized by long time constants, memory effects, and highly non-linear behavior. Due to the variety of different phenomena that have been observed, as well as the large number of parameters involved and the analytical intractability of the equations describing the non-steady-state, very little work has been done to characterize or model transient behavior without recourse to empirical description. Understanding transient phenomena, however, remains an extremely important goal because the application of photoconductors dictates that they are most often used in a transient fashion. Low background astronomy observations are done using low frequency chopping to allow for background subtraction and absolute calibration of the size of signals. Transient behavior that is characterized by long time constants limits the speed of the detector, extends the required observing time for a given sensitivity, and limits the detector ac responsivity.

Ge:Be and Ge:Zn detectors have been shown to display, within a certain temperature range, a characteristic transient response to changes in photon flux illumination rates that is characterized by time constants on the order of seconds. In this paper, an experimental study of the transient behavior, as a function of temperature, electric field, photon flux rate, photoconductive gain, and materials parameters, will be presented.

Ge:Be and Ge:Zn Photoconductors

Beryllium occupies a substitutional site and is a double acceptor in Ge with ionization energies of 24.8 and 58 meV (1). Interest in Ge:Be as a detector material is generally limited to the first ionization stage, and the earliest evaluation of Ge:Be photoconductors was published by Shenker, Swiggard, and Moore in 1967 (2). Recent development of Ge:Be has been directed toward producing an optimized detector in the 30-50 μm wavelength range (3).

Zinc is also a double acceptor occupying a substitutional site in Ge, with ionization energies of 33 and 86.5 meV (4). Ge:Zn detectors were developed in the early 1960's, but were never extensively utilized (5,6). There is less practical application for Ge:Zn detectors in astronomy, since they begin to overlap the wavelength range which can be covered by Si:X detectors and since the optimization of Ge:Be detectors has been quite successful. Our interest in Ge:Zn is primarily as an analogous system to Ge:Be, since both materials contain a semi-deep primary dopant (Be or Zn) as well as residual shallow level impurities.

A schematic spectral response including Ge:Be and Ge:Zn is shown in Fig. 1. In most studies concerned with the characterization of these far-IR detectors for astronomy-related work, only the first hole is removed (i.e., first ionization state) and the doubly ionized state is never present. This is accomplished by operating the device at low temperatures and using appropriate filtering so that there is neither thermal nor optical energy to remove a second hole. The compensating donor concentration is always low enough ($N_D \ll N_{Be}$) so that no doubly ionized centers are formed due to compensation.

Transient Response of Extrinsic Photoconductors

A simple model for the transient response of an extrinsic photoconductor can be derived for low background operation if one assumes a space charge neutral detector and neglects all contact effects (7). In this case, the rate equation for the change in free holes is given by

$$\frac{dp}{dt} = Q + N_V \langle v \rangle \exp \frac{E^f - E^v}{(kT)} N_i^0 \sigma - \langle v \rangle \sigma p (N_D + p)$$

The first term corresponds to the optical generation, the second to the thermal generation and the last to recombination. Q is the hole generation rate, N_V is the valence band density of states, $\langle v \rangle$ is the average thermal velocity, $E^f - E^v$ is the Fermi level referenced to the valence band, N_i^0 is the concentration of neutral acceptors, and σ is the recombination cross section. This expression assumes that optical and thermal generation and cascade capture recombination are the dominant processes in the material, neglecting other effects such as impact ionization, radiative recombination, and Auger recombination. This is a very good approximation for low background photoconductors operated at fields below the breakdown field.

This rate equation can be written as

$$dp/dt = g - p/\tau$$

where g is the sum of all generation terms and $\tau = (\sigma v N_D)^{-1}$ since $N_D \gg p$ for low background flux. If we increase g by an amount Δg then

$$d\Delta p/dt = \Delta g - \Delta p/\tau$$

For the case in which Δg arrives as a step pulse ($\Delta g = 0$ for $t < t_0$, $\Delta g = \text{constant}$ for $t > t_0$) one finds:

$$\Delta p = \Delta g \tau [1 - \exp(-t/\tau)] \quad (4.4)$$

Since for low background work τ is not generally a function of the photon flux, this model predicts that the transient response should be given by the lifetime of free carriers in the device and should be symmetric with regard to growth or decay for small changes in photon flux. It is from this model for transient response that one derives the standard relationship between lifetime, compensation, and detector bandwidth.

Effects of Space Charge and Non-linear Behavior

Although it is of general use in predicting first order behavior, the simple linear model for the space charge neutral photoconductor fails to explain many of the phenomena which are observed during operation. This is not too surprising since photoconductors are actually non-linear devices which are not space-charge neutral. Non-linear behavior arises because the coefficients for recombination or impact ionization processes are actually strong functions of electric field. Space-charge regions exist near both contacts and may, under some circumstances, exist in the bulk as well.

One of the earliest models for space charge related effects on transient behavior was proposed by Williams in 1969 (8). He observed a slow component

($\tau \gg \tau_{\text{lifetime}}$) in the response of Ge:Hg photoconductors under conditions where the photoconductive gain was greater than unity. This was attributed to the "sweep-out" of carriers generated by external illumination, leading to a space charge region in the device. Since the relaxation of the space charge was theoretically shown to occur with a time constant of $\rho\epsilon\epsilon_0$ (the product of resistivity and the dielectric constant), the term dielectric relaxation has since been applied to this phenomena.

The theory of carrier sweep-out and dielectric relaxation assumes a restrictive boundary condition ($\Delta p = 0$ at the anode) so that no free carriers are immediately available for injection. In this case, when a pulse of light is incident upon the device, free carriers Δp will be produced and will move toward the cathode under the effect of the applied field. Near the anode, a concentration $\Delta N_A^- = \Delta p$ of ionized acceptors will be left. This space charge layer will produce an electric field gradient which acts to neutralize the space charge region. The space charge region is neutralized with a time constant proportional to the resistivity of the material, i.e.,

$$\Delta N_A^-(t) = \Delta N_0^- \exp(-t/\tau) \text{ where } \tau = \epsilon\epsilon_0/(\mu\rho_0e) = \epsilon\epsilon_0\rho_0$$

This theory has been cited extensively when long time constants are observed in extrinsic photoconductors. Its greatest success has been in explaining the rolloff of photoconductive gain as a function of frequency for high resistivity detectors with the more advanced forms of the theory (9,10). However, there are several limitations to the model. The most important is the assumption of a boundary condition of $\Delta p = 0$ at the anode. This means that no free holes are readily available for injection at the contact. This requires further justification, especially in the case of an ohmic, ion-implanted contact which serves as a reservoir for free carriers even at very low temperatures. A restrictive boundary condition is a requirement for sweep-out to occur, and the fact that some behaviors are well described by the dielectric relaxation theory indicates that contact behavior may not be perfectly ideal and that contact behavior and space charge effects are important in transient behavior.

In 1959 Lampert and Rose published a phenomenological analysis of the transient behavior of ohmic contacts (11) and also proposed that the response time of a photoconductor for current transients could, under certain circumstances, be determined by the readjustment of the space charge barrier at the contact. More recent developments in contact modeling will be discussed in Part IV.

EXPERIMENTAL

The Ge:Be and Ge:Zn photoconductors were fabricated from slices taken from ~1 kg Czochralski-grown single crystals. The concentrations of both the primary dopant (Be or Zn) and the residual shallow impurities (B, Al, P) were determined from variable temperature Hall effect measurements. Beryllium and zinc concentrations ranged from 10^{14} to 10^{15} cm^{-3} . The shallow residual impurity concentration ranged from 10^{11} - 10^{12} cm^{-3} , with the shallow residual acceptor concentration exceeding the residual donor concentration.

Slices of ~1 mm were cut perpendicular to the crystal growth axis ($\langle 113 \rangle$ for most cases considered here). The thickness of the slice was determined by the desired inter-electrode distance and varied over a range from 0.2 to 3.0 mm. One mm was the standard value for all results unless otherwise

stated. The slices were lapped with No. 600 SiC grit to remove saw damage. The wafer surfaces were etched in a 4:1 mixture of HNO₃:HF, rinsed with electronic grade methanol, and dried with boil-off N₂. Immediately prior to implantation, the Ge slice was immersed in 1% HF to remove surface oxide. Boron implanted layers (1×10^{14} cm⁻², 25 keV and 2×10^{14} cm⁻², 50 keV) were used to provide degenerately doped p⁺ contacts at low temperatures (12). Layers of Ti or Pd (500 Å) and Au (8000 Å) were deposited by Ar sputtering to protect the implanted layer and provide areas for electrical contacts as well as mechanical mounting. After metallization, the finished slices were heated to 300°C for approximately one hour under Ar gas to anneal damage from the implantation and relieve stress in the metal layers.

Final devices of desired geometry were cut from the finished wafer. A common detector size was $1 \times 1 \times 3$ mm³ with 1 mm between the contacts. The bare detector surfaces were etched as previously described. The Au layer is not attacked by the etchant. Detectors were either soldered with pure In or glued using a silver-loaded epoxy to a 1 mm diameter carbon steel shaft and then mounted inside a brass integrating cavity with a 1 mm aperture. Integrating cavities are often used in the testing of Ge detectors because of the small value of the absorption coefficient which leads to a small quantum efficiency for single pass configurations.

The detectors were evaluated in a specially designed cryostat. A liquid helium space with a volume of approximately one liter is shielded with a liquid nitrogen temperature jacket. A common vacuum space provides thermal insulation as well as an evacuated space for the detector. The working area is a thick copper plate in contact with the liquid helium bath. The detector in its cavity and all its surroundings are heat sunk to this plate with screws and pure In foil.

The photon signal incident upon the detector is produced externally and cold-filtered within the dewar. An external Au-plated metal chopper is used to switch the IR source between variable temperature blackbodies. Most commonly the signal was produced by chopping between a 77 K blackbody (immersed in LN) and the 300 K radiation from the back wall of the chopper box. An Electro-Optical* blackbody source (Model 311) with a temperature range of 20 - 1000°C was also used as a radiation source. Inside the dewar, a rotating wheel with a mechanical connection to the outside allows an internal aperture ($\phi = 1$ mm) to be opened and closed.

The low background condition for detector testing is achieved with a combination of reduced filter transmission and the geometrical factor imposed by the size of the apertures and the distance between them. The narrow band filter trains consist of Fabry-Perot mesh filters and Reststrahlen salt filters (13). The combined filter trains had bandwidths of ≈ 1 μ m centered at 36 and 42 μ m for use with Ge:Zn and Ge:Be respectively. The filters are independently mounted along the optical axis on sliding baffles and are heat sunk directly to the copper plate by two screws and pure In foil.

The detector is located inside its integrating cavity at the far end of a Cu box. Special care was taken to make the box light tight. A double cover with a meandering pump-out groove was used, and all surfaces within the box

*Reference to a company or product name does not imply approval or recommendation of the product by the University of California, the U. S. Department of Energy, or the National Aeronautics and Space Administration to the exclusion of others that may be suitable.

are covered with 3M flat black paint so that, with the shutter aperture closed, the detector should see no other radiation than the 4K blackbody radiation of its surroundings. The glass feedthrough for the detector leads is opaque to far-IR radiation.

The photoconductor signal is amplified by a standard transimpedance amplifier (14). The input stage consists of two matched junction FETs (J230 selected by Infrared Laboratories, Tucson, AZ). The JFETs are located inside a light-tight Cu housing with opaque feedthroughs. They are mounted off the liquid helium temperature plate on a thin wall fiberglass tube. A 1 k Ω resistor is glued with epoxy to the JFETs. A constant voltage applied across the resistor together with the power dissipated by the JFETs keeps the operating temperature at approximately 77 K.

The transient response of Ge:Be and Ge:Zn detectors to a step increase in photon flux was studied over a wide range of parameters. The change in signal was caused by manually moving a reflecting gold plated shutter which switched the detector field of view from the 77 to the 300 K blackbody source. The flux levels and flux change are given in Table 2. It is clear that, since $\Delta p > p_0$, this is not a case of small signal response. It is an experimental condition, however, which does correspond to what the detectors often see in practice. The speed at which the shutter was opened was approximately 20 msec. Although this is a long time relative to the free carrier lifetime, we will see that it is very short compared to the time constants which were observed.

RESULTS

The transient response which was observed in these materials is shown, as a function of temperature, in Fig. 2 for Ge:Zn and Fig. 3 for Ge:Be. This shows the detector output (i.e., detector current versus time) in response to a step increase in photon flux. The detector response consists of both a slow and a fast component. This can be seen more clearly by considering the compiled data for the Ge:Zn case in Fig. 4. One sees that the magnitude of the fast component increases only slightly with increasing temperature, while the slow component increases much faster. The time constant of the slow response, taken as the point where the slow component reaches 63% of its full value, ranges from < 0.1 sec (the shortest time which could be detected experimentally) to greater than 5 sec for Ge:Zn and from < 0.1 sec to 2 sec for Ge:Be. The detector response was symmetric when comparing the result for the increase in flux and the corresponding decrease in flux to return to the original background.

Temperature

The time constant of the slow component decreases with increasing temperature and has been plotted as a function of inverse temperature in Fig. 5. The activation energy associated with the slope is approximately 2.5 meV for the Be case and 3.2 meV for Ge:Zn. Note that this energy does not correspond to any of the ionization energies of the known elemental dopants in the material. These activation energies have been found to be relatively insensitive to changes in detector bias or material doping, differing only by several tenths of an meV for different devices.

Because an increase in detector temperature necessarily implies an increase in free hole concentration (due either to increased thermal generation or to longer free carrier lifetime), it was necessary to determine if the faster time

constant with increasing temperature was actually due to increasing lattice temperature or the resultant increase in free hole concentration. In order to separate these two effects, a separate blackbody photon source (a 1 k Ω resistor) was placed in the dewar within the field of view of the detector. The temperature of this source could be varied externally. Temperature changes at a constant flux could then be compared to the effect of photon background changes at a constant temperature, with both effects causing the same change in free hole concentration in the device.

The results of this experiment are presented in Fig. 6 for a Ge:Be detector. One sees that the decrease in time constant is due to the change in lattice temperature and not to the increase in background hole concentration. The effect of increasing hole concentration is weak, if any, over the measured range. Thus, the time constant is not directly proportional to detector resistivity, an important indication that dielectric relaxation is not determining the transient behavior.

Electric Field

The time constant of the symmetric slow response did not vary with increasing electric field over a range from 1.0 to 6.0 V/cm. The amplitudes of both components as a function of bias are plotted in Fig. 7. Both increase with increasing field and there is no evidence of saturation of the fast component, as might be expected for sweep-out mechanisms. The fast component displays a linear response at low fields and approaches a V^2 dependence as the field is increased and carrier heating occurs. This is the standard I-V behavior of extrinsic photoconductors. The slow component, in contrast, displays a super-linear voltage dependence even at low bias.

Intercontact Distance and Contact Area

The effect of the intercontact distance on the slow component response was studied by varying the intercontact distance over a range from 2.5 to 0.2 mm in detectors made from Ge:Be crystal No. 719-11.6. This has the effect of changing the photoconductive gain ($G = \mu\tau E/L$) by a factor of 12.5 if detectors are evaluated at a constant field, V_{bias}/L . The results are tabulated in Table 2 for three different temperatures at a constant field of 1 V/cm. One sees that, at a constant temperature, the time constant of the slow response is independent of photoconductive gain within the measured range.

The time constant of the slow response was also evaluated as a function of contact area to determine the effect of current density through the device for a fixed mobility, lifetime, and photoconductive gain. This was accomplished by testing detectors with varying cross-sectional area (1 x 1, 1 x 3, 3 x 3 mm²) in similar integrating cavities under the same photon flux. If one assumes that the number of photons absorbed is constant in the cavity, then the total current must be constant and the current density will scale inversely to detector area.

The effect of increasing contact area is illustrated by the oscilloscope traces in Fig. 8. With large area contacts, an additional slow component appeared in the response. This component was more pronounced for the increasing current transient than for the decay, as indicated by Figs. 8c and 8d. In Fig. 9, theoretical curves based on two exponentials, with $\tau_2 \gg \tau_1$ were used to fit the transient response. The appearance of an additional slow component is evident in the deviation from the two exponential fit for the large area

case. One cannot conclude that the time constant increases with contact area; it simply can no longer be described as:

$$S_t = S_1[1 - \exp(t/\tau_1)] + S_2[1 - \exp(t/\tau_2)]$$

One effect of increasing the detector size under fixed conditions of illumination is that the near-contact illumination becomes increasingly non-uniform. Non-uniform illumination of contacts or of the photoconductor has previously been shown to cause anomalous behavior in extrinsic photoconductors (15). To determine the effect of uniformity of contact illumination, and to determine if the long time constant behavior observed in all the photoconductors was due to that effect, a detector was made in which the contacts were uniformly illuminated. This was done by making a thin detector with contacts on the backside and using front side illumination. This would fully illuminate the front side region and the contact regions. The transient response associated with this detector was included as Fig. 9a, and one sees that a long transient response still exists, but that it can be fit very well with a two time constant model.

The appearance of the additional slow component for the large area side-illuminated device makes it difficult to obtain a good value of the time constant for the slow component which is common to all detectors. The values for τ and current density J are given in Table 3 for the thin detector, the $1 \times 1 \text{ mm}^2$, and the $1 \times 3 \text{ mm}^2$. The slightly longer time constant for increasing contact area may be due to the additional slow component since a two time constant model was assumed in all the fits and is clearly not correct even for the $1 \times 3 \text{ mm}^2$ cases. The conclusion of the effect on τ of current density, then, is that τ is either independent or very weakly dependent on current density, since J varies by a factor of 15 while τ varies by less than a factor of two in all cases for a constant temperature.

Material Parameters

Although all of the Ge:Be and Ge:Zn photoconductors tested under low background conditions (as well as all Ge:Ga detectors, which have also been studied extensively) display "slow" transient behavior, the relative amplitudes and response times of the slow components vary greatly in different materials. Because contact fabrication was the same for all the detectors, this indicates that the bulk material doping, whether in the bulk or in the near-contact region, is a critical parameter in transient behavior.

The materials dependence of the transient response appears to be a complicated function of many parameters. First, slow components with large amplitudes ($> 10\%$ of the total signal) are only observed in materials grown under a gas ambient: Ge:Zn grown under N_2 and H_2 atmospheres and Ge:Be grown under a H_2 atmosphere. Ge:Be crystals grown under vacuum did not show this behavior. Secondly, the slow component was most prominently present in closely compensated crystals ($N_A(\text{shallow}) = N_D$) and increased in amplitude with increasing degree of compensation. In the Ge:Zn material, however, the slow component disappeared when the shallow acceptors were completely compensated [i.e., $N_D > N_A(\text{shallow})$]. Extensive annealing of the Ge:Zn and Ge:Be material, at temperatures sufficient to remove H through out-diffusion, did not affect the transient behavior.

It is apparent from the collection of data that the materials dependences of the phenomena are relatively complicated, since the crystals do not vary

greatly in terms of either primary or shallow level doping and there are many parameters combinations to be considered. Deep level transient spectroscopy studies were done along the length of Ge:Zn crystal in which the slow transient behavior became increasingly dominant in a series fabricated from slices taken at increasing distance from the seed end of the crystal. This was done to determine if the appearance of any deep levels would be coincident with the appearance of the large slow transient response. No deep levels were detectable at any point, however, down to a limiting concentration of $\approx 10^{10}$ cm⁻³, equivalent to 1% of the shallow level doping.

Lifetime Measurements

Measurements of free carrier lifetime as a function of photon flux were made to determine if the slow transient response was caused by an increase in lifetime with increased illumination. This was tested in the following way. The transient response of the detector to a step function increase in photon flux was measured to determine the amplitude and speed of the response. Then, while maintaining the higher flux level as the new background, an additional signal Δp of the same size as the previous signal was imposed. In this way it was possible to determine the responsivity at each level of background flux. The responsivity is a function only of lifetime for a given detector at fixed electric field and temperature. Results of the experiment are summarized in Fig. 10.

One sees that the photoconductive gain did not increase at the higher flux level, but in fact decreased by $\sim 20\%$. This could be a real effect but is more likely due to the uncertainty ($\pm 20\%$) in the calculation of the photon flux which requires mixing the effects of the blackbody source and the room temperature emission from the window. If the slow component were due to an increase in lifetime, however, one would expect an increase of a factor of 2 - 3 in responsivity since this is the increase in responsivity due to the slow component in the transient, and this is clearly not observed. This result also confirms earlier results showing that the time constant τ is not directly proportional to the background hole concentration. The decrease that was noted in τ (\sim a factor of 1.5) may reflect a weak dependence on background flux or the heating of the detector that occurs when the field of view of the dewar is filled with the hot external blackbody. This heating is known to occur because the reading of the temperature sensing resistor indicates a temperature rise when the radiation from the hot blackbody enters the dewar.

DISCUSSION

To summarize the experimental results: we observe a temperature dependent transient behavior in Ge:Be and Ge:Zn photoconductors with time constants on the order of seconds. The time constant is not dependent on electric field, material resistivity, or photoconductive gain. There are material dependences, and the phenomena is observed only in samples in which the shallow residual impurities are closely compensated.

A survey of time constants associated with the measured transient behavior, free carrier lifetime, and dielectric relaxation time for the Ge:Zn and Ge:Be detectors is presented in Table 4. Free carrier lifetimes, τ_1 , were determined from measured dc responsivity values, while the dielectric relaxation time constant, τ_p , can be determined directly from a measurement of detector

resistance and geometry, i.e.,

$$\tau_1 = R\epsilon\mu E / (h\nu L) \quad (R = \text{responsivity})$$

and

$$\tau_0 = \rho\epsilon\epsilon_0.$$

The comparison between these time constants shows that the observed response is orders of magnitude longer than both the dielectric time constant and the lifetime. This conclusion is also supported by a number of experiments. The difference in the effect of increased background flux versus increased temperature (Fig. 5) showed that what is important is not the resistivity or the concentration of free holes, but rather the lattice temperature of the device. Dielectric relaxation, in contrast, is resistivity dependent. Also, dielectric relaxation theory predicts that the fast component should saturate with increasing bias once sweep-out effects begin. This is also not the case here, as Fig. 6 has shown. The first conclusion, therefore, is that the observed response cannot be attributed to a lifetime controlled or dielectric relaxation controlled process.

The correlation between the appearance of the slow component and close compensation of many of the samples is probably affected by the strong dependence of free carrier lifetime on shallow level compensation in these multi-level systems (16,17). The strong temperature dependence of the amplitude of the slow component is explained by the free carrier lifetime increase as a function of temperature that has been observed in the Ge:Be and Ge:Zn detectors (3,18). Since the lifetime is known to be increasing rapidly in the temperature ranges where the transient is observed, one could posit that the τ of the response is proportional to the free carrier lifetime which is determined by the distribution of trapped charge between the shallow and semideep levels. It is important to distinguish between temperature dependence and flux dependence of the lifetime. Results showing that the lifetime is not increasing with increased flux indicate that the transient itself is not a result of increasing lifetime. The total amplitude of the signal, however, is explained by the close compensation of the material.

The analysis of annealed samples for several of the detectors (719-5.6, 719-11.6, 715-10.4) was performed to determine if the outdiffusion of H₂ or any other trapped gases affected the transient response. This question arose in view of the fact that the relative amplitude of the slow component was largest in crystals grown under a H₂ or N₂ atmosphere. In all cases where the annealing behavior did not greatly affect the shallow level compensation, the transient behavior was unchanged after annealing. One concludes that the H and H-related centers which have been shown to exist in the materials and demonstrated to anneal away at these temperatures (19) do not play a major role in the transient behavior.

The temperature dependence of the time constant of the transient response can be analyzed from several perspectives. The "activation energy" associated with the time constant (~ 2.5 meV for Ge:Be, ~ 3.2 meV for Ge:Zn) indicates an effect involving shallow levels or contact behavior rather than the primary dopant levels or the presence of deep levels. Although energies of < 5 meV do not correspond to any known elemental dopants, one must remember that an illuminated photoconductor is not simply in thermal equilibrium and that the Fermi level is actually given by a quasi-Fermi level which, at low temperatures, is determined entirely by the photon flux.

Figure 11 shows the position of the quasi-Fermi level and the thermal equilibrium Fermi level in the dark as a function of temperature for the parameters listed. One sees that the quasi-Fermi level is less than the ionization energy of the shallow levels for the temperatures and photon fluxes at which the photoconductors operate. The quasi-Fermi level also increases with increasing temperature for a given flux, which may explain why a higher "barrier" is measured for Ge:Zn than for Ge:Be. More importantly, the only place in the device where barriers might exist which are related to the quasi-Fermi level is in the near contact region. This is the first experimental evidence pointing to near-contact behavior as the source of the slow transient response.

We have also considered the possibility that the shallow A^+ centers, Be^+ and Zn^+ , may play a role in determining the current transient behavior. These over-charged acceptor centers have binding energies of < 5 meV (20,21). This does not explain, however, why this behavior is not found in all Be- and Zn-doped detectors. More importantly, the slow transient behavior in Ge:Zn detectors is observed between 5 and 10 K, and the equilibrium concentration of the Zn^+ center at those temperatures will be very small.

Other experiments were designed to isolate the transient response as a near-contact or bulk phenomena. The current in the photoconductor, neglecting diffusion terms, is given by

$$J = pe\mu E + \epsilon dE(x,t)/dt$$

or

$$dJ/dt = e\mu E dp/dt + e\mu p dE/dt + \epsilon d^2E/dt^2$$

Current transients, therefore, must arise due to transient changes in either electric field or hole concentration. Since the hole concentration in the bulk of the sample is given by $p = \dot{p}\tau$, changes in free hole concentration in the bulk will only occur if there is a change in free carrier lifetime, neglecting sweep-out effects. The experimental results showing that the free carrier lifetime is not increasing with increasing illumination (Fig. 10) indicates that the dp/dt term can be neglected to first order, and that the current transient must arise from slow transients in the electric field. Because the profile of the electric field in a photoconductor is determined mainly by trapped space charge near the contact, this is a second argument in support of the idea that the slow transient is not a bulk effect.

Contact Behavior

Very little attention has been given to low temperature ohmic contacts, both because of their limited use and the mathematical complexity of including contact effects in the transport equations. Recently, however, some attempts have been made to solve the differential equations describing steady state carrier transport, including the boundary condition for an ideal ohmic contact (22). An ohmic contact is generally defined as a metal-semiconductor contact that has a negligible resistance compared to the resistance of the bulk material. According to Sze, an ohmic contact is one that "should not significantly perturb device performance. . . and can supply the required current with a voltage drop that is sufficiently small compared with the drop across the active region of the device" (23). One method of achieving this is to form, either through diffusion, implantation, or alloy regrowth, a heavily doped surface layer in the semiconductor. Carriers can then tunnel through the metal-semiconductor barrier and the ability of the contact to supply carriers will be independent of the barrier height ϕ_B .

Most of the data on ohmic contacts are for room temperature contact to Si and III-V and II-VI devices, where either a low barrier height or a tunneling contact will lead to ohmic characteristics. For cooled IR photoconductors, however, the available thermal energy is very small (0.36 meV at 4.2 K), so the contact must be a tunneling contact. The impurity concentration in the heavily doped layer must be high enough to exceed the metal-semiconductor transition, i.e., the Fermi level must lie within the valence band at all temperatures for ohmic contact to a p-type device. This will lead to a reservoir of free holes in the semiconductor and the carriers can move through the metal-semiconductor barrier at any temperature.

The free carriers in the contact region do not diffuse throughout the semiconductor bulk because there is an additional diffusion barrier $E_y - E_f$ which exists due to the space charge generated when free holes diffuse into the bulk near the contact and are trapped by ionized acceptors. This leads to a region of trapped space charge in the near-contact region. The barrier is shown in Fig. 12, which displays the space charge, electric field, potential, and the energy band diagram for the near-contact region with and without an applied field. A linear distribution of ρ has been assumed only for schematic simplicity. This figure shows that there is a point where the potential energy goes through a maximum for holes. This occurs at the point where the electric field is equal to zero, a point of pure diffusion current. The small barrier for free holes from the implanted region to the bulk is usually neglected in discussions of ohmic contacts because in most cases it is small compared to the thermal energy at room temperature. It is not immediately clear, however, that this can be neglected in a device operated at 4 K. When one speaks, therefore, about the contact barrier in an extrinsic Ge photoconductor, one is usually not referring to the metal-semiconductor barrier, which is assumed to be negligible due to the tunneling contact, but rather to the small diffusion barrier in the material itself.

The physics of the near-contact region is dominated by the space charge which exists due to the diffusion of free holes from the contact into the bulk material. This occurs because of the large concentration gradient between the implanted layer ($p \sim 10^{20} \text{ cm}^{-3}$) and the bulk material ($p < 10^2 \text{ cm}^{-3}$ under low background operating conditions). Like the diffusion of electrons and holes across a p-n junction, this process is counteracted by the build-up of a space charge region. At low temperatures, the free holes will be trapped (i.e., recombine into the ground state) on the ionized acceptors which are present due to compensation, leading to the build-up of a positive space charge.

Westervelt and Teitsworth (22) have constructed a simplified two-region model (near-contact and bulk) which is valid only on a long time constant scale. They predict slow transient responses on the order of ≈ 1 second, although the status of the modeling at this point leaves unanswered questions concerning the relative magnitude of the predicted slow response or the effect of close compensation in a multilevel system. A physical phenomena in the device is identified, however, which is occurring on a time scale much longer than the free carrier lifetime or the dielectric relaxation time.

The experimental results presented here are not fully explained by the current models for transient behavior in extrinsic photoconductors. The most important question remaining is why the amplitude of the slow component can be such a large part of the total signal in certain closely compensated Ge:Be and Ge:Zn materials. This will require development of a model for multilevel systems which includes the residual shallow impurities, as well as semideep primary dopants such as Be or Zn, since the compensation of these levels seems

to play a large role in determining device behavior. Also, the temperature dependence of the slow transient response, and its relative insensitivity to other variables such as free hole concentration in the bulk, bulk electric field, and photoconductive gain, indicates a thermally activated barrier-related phenomena in a region, such as the contact region, where the free hole concentration and electric field are not greatly affected by changes in the bulk values of these parameters.

SUMMARY

Transient behavior with respect to changes in incident photon flux levels has been observed to occur in both Ge:Be and Ge:Zn photoconductors with time constants ranging from 0.1 to greater than 5.0 seconds. A comparison of time constants associated with free carrier lifetime, dielectric relaxation, and the measured transient response indicates that the transient response is several orders of magnitude longer than either dielectric relaxation or lifetime and is therefore limited by some other phenomena in the device. Experimental results showing a strong dependence of the transient behavior on device temperature, coupled with insensitivity to bulk phenomena such as free hole concentration and electric field, indicate that the adjustment of space charge in the near contact region may be determining the transient response.

ACKNOWLEDGMENT

This work was supported in part by NASA Contract No. W-14,606 under Inter-agency Agreement with the Director's Office of Energy Research, Office of Health and Environmental Research, U.S. Department of Energy under Contract No. DE-AC03-76SF00098.

REFERENCES

1. Cross J W, Ho L T, Ramdas A K, Sauer R and Haller E E, Phys. Rev. B 28, 6953 (1983).
2. Shenker H, Swiggard E M and Moore W J, Trans. Met. Soc. AIME 239, 347 (1967).
3. Haegel N M, Haller E E and Luke P N, Intl. J. Infrared and Millimeter Wave 4, 945 (1983).
4. Ramdas A K and Rodriguez S, Repts. on Progress in Physics 44, 1297, (1981).
5. Picus Gerald S, J. Phys. Chem. Solids 22, 159 (1961).
6. Levinstein H, Appl. Opt. 4, 639 (1965).
7. Bratt P R, "Impurity Germanium and Silicon Infrared Detectors" in: Semiconductors and Semimetals, Willardson R K and Beer A C eds. (New York: Academic Press) 12, 62, 1977.
8. Williams R L, J. Appl. Phys. 40, 184 (1969).
9. Milton, A Fenner, Appl. Phys. Lett. 16, 285 (1970).
10. Milton, A Fenner and Blouke M M, Phys. Rev. B 3, 4312 (1971).
11. Lampert M A and Rose A, Phys. Rev. 113, 1236, (1959).
12. Haller E E, Hueschen M R and Richards P L, Appl. Phys. Lett. 34, 495 (1979).
13. Watson D M, Ph.D. Thesis, University of California, Berkeley, 1982.
14. Low F J, SPIE 280, 56 (1981).
15. Sayre C, Arrington D, Eisenman W and Merriam J, Opt. Eng. 16, SR-40 (1977).
16. Alexander D H, Baron R and Stafsudd O M, IEEE Trans. Elec. Dev. ED-27, 71 (1980).
17. Geim K, Pensl G and Schultz M, Appl. Phys. A 27, 71 (1982).
18. Haegel N M, Ph.D. Thesis, University of California, Berkeley, 1985.
19. McMurray Jr, R E, Haegel N M, Kahn J M and Haller E E, Solid State Comm. 53, 1137 (1985).
20. Haller E E, McMurray Jr, R E, Falicov L M, Haegel N M and Hansen W L, Phys. Rev. Lett. 31, 1089 (1983).

21. Haller E E, McMurray Jr, R E, Falicov L M and Haegel N M, "Positively Charged Acceptors with $(1s)^3$ and $(1s)^4$ Configurations" in: Proc. 17th Intl. Conf. on the Physics of Semiconductors, Chadi J D and Harrison W A eds. (Springer) 679, 1985.
22. Westervelt R M and Teitsworth S W, J. Appl. Phys. 57, 5457 (1985).
23. Sze S M, Physics of Semiconductor Devices, 2nd ed. (New York: John Wiley and Sons, Inc.) 304, 1981.

FIGURE CAPTIONS

- Fig. 1. Schematic spectral response for Ge:Be and Ge:Zn.
- Fig. 2. Transient response of Ge:Zn detector at $T =$ a) 5.2 K, b) 6.3 K, c) 7.3 K, d) 8.4 K and e) 9.0 K.
- Fig. 3. Transient response of a Ge:Be detector at $T =$ a) 2.5 K, b) 2.6 K, c) 2.7 K, d) 2.8 K and e) 2.9 K.
- Fig. 4. Compiled data from Fig. 3 showing the effect of increasing temperature on signal size.
- Fig. 5. Time constant of the slow component as a function of inverse temperature.
- Fig. 6. Time constant for the slow component as a function of background hole concentration, where the hole concentration was changed by changing A) temperature and B) background flux.
- Fig. 7. Amplitude of fast and slow component as a function of bias.
- Fig. 8. Detector response as a function of device area with constant photon fluence. Arrows indicate final steady state value of the response. Final picture shows the effect of decreasing the illumination level.
- Fig. 9. Transient response of four Ge:Be detectors to increased illumination: from left, a) fully illuminated contact, b) $1 \times 1 \text{ mm}^2$, c) $1 \times 3 \text{ mm}^2$ and d) $3 \times 3 \text{ mm}^2$. Solid lines represent a calculated response with two time constants. Note the additional slow component appearing in the large area detectors.

Fig. 10.

$T_{\text{background}}$	77 K	300 K
	$1.5 \times 10^8 \text{ p/s}$	$8.9 \times 10^8 \text{ p/s}$
T_{signal}	300 K	497 K
	$8.9 \times 10^8 \text{ p/s}$	$1.6 \times 10^9 \text{ p/s}$
Signal (Δ)	$7.4 \times 10^8 \text{ p/s}$	$7.1 \times 10^8 \text{ p/s}$
Responsivity (A/W)		
1 V/cm	0.53	0.44
6 V/cm	7.9	5.8
τ (sec)		
1 V/cm	1.6	1.1
6 V/cm	1.7	1.2

- Fig. 11. Calculated Fermi levels for illuminated and nonilluminated material with: $N_{\text{Be}} = 5 \times 10^{14} \text{ cm}^{-3}$, $N_{\text{A}} = 10^{12} \text{ cm}^{-3}$, $N_{\text{D}} = 5 \times 10^{11} \text{ cm}^{-3}$, $\sigma = 1 \times 10^{-12} \text{ cm}^2$, $Q = 5 \times 10^{10} \text{ p/s}$.
- Fig. 12. Space charge, electric field, potential and band diagram as a function of distance in the near-contact region A) without applied external bias, and B) with applied external bias.

TABLE 1

Photon Flux Levels for Transient Measurements

Detector	Ge:Be	Ge:Zn
λ (μm)	42	36
Background flux(p/s)	1.5×10^8	1.5×10^8
Bkgr. + signal (p/s)	8.9×10^8	1.1×10^9
Signal Δ (p/s)	7.4×10^8	9.2×10^8

TABLE 2

Time Constant as a Function of Intercontact Distance

<u>L (mm)</u>	<u>τ^* (sec)</u>		
	T = 2.6 K	2.73 K	3.0 K
0.2	1.1	0.4	0.15
1.0	0.9	0.4	0.2
2.5	1.0	0.45	0.10

* all values \pm 0.1 second

TABLE 3

Time Constant as a Function of Current Density

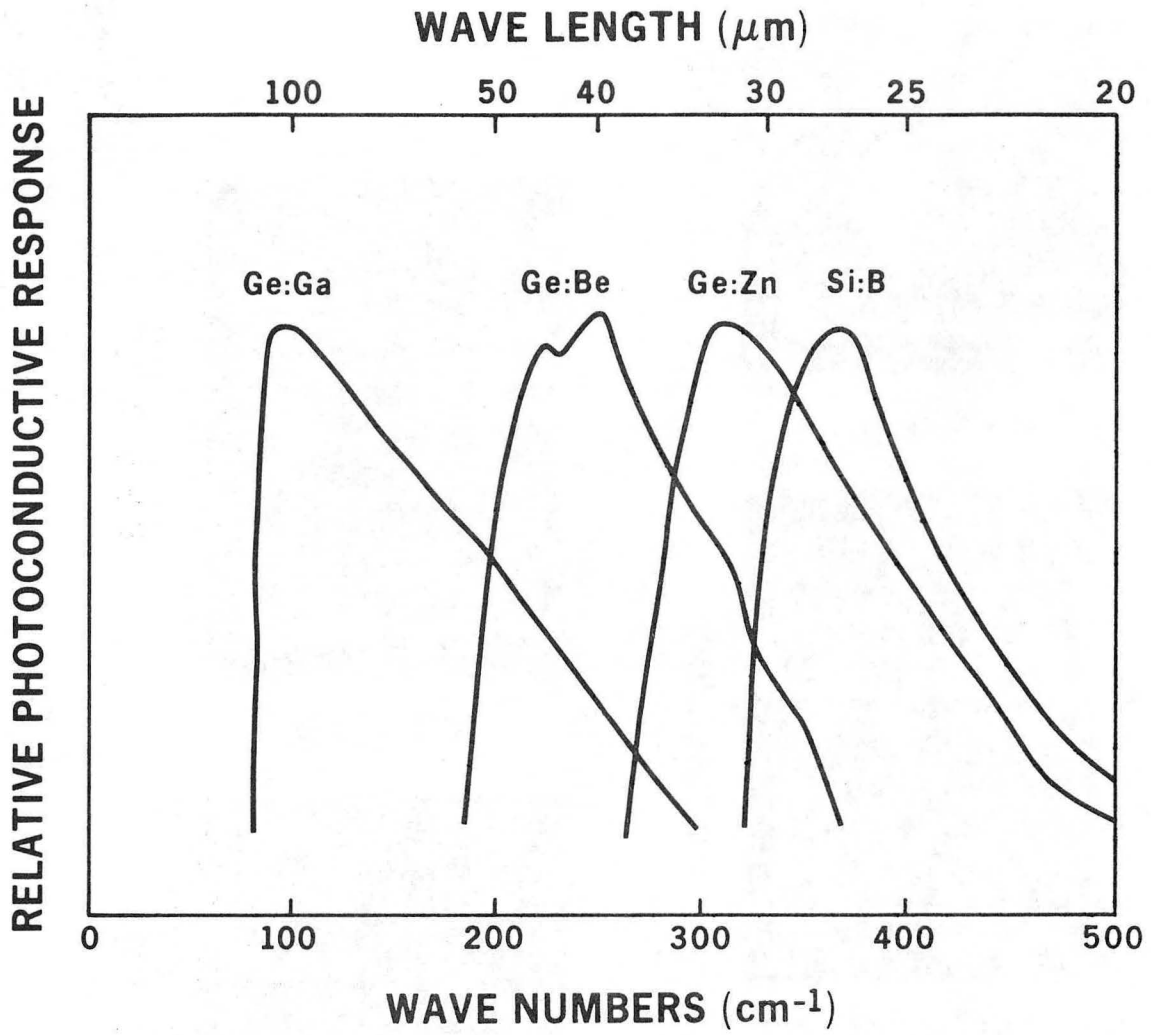
<u>Detector Area</u> <u>(mm²)</u>	<u>J</u> <u>(arb. units)</u>	<u>τ^*</u> <u>(seconds)</u>		
		T = 3.0 K	2.73 K	2.60 K
0.2	15	0.2	0.4	0.8
1.0	3	0.2	0.4	0.9
3.0	1	0.3	0.5	1.1

* all values \pm 0.1 seconds

TABLE 4

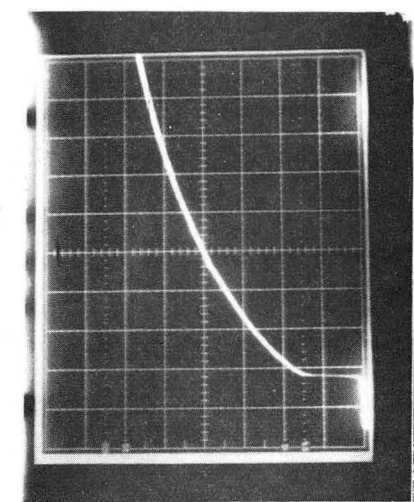
Survey of Detector Time Constants

	τ lifetime (sec)	τ_p (sec)	τ slow component (sec)
<u>Ge:Be</u>			
T = 2.7 K E = 1 V/cm	3×10^{-9}	2.8×10^{-2}	1.6
T = 2.7 K E = 6 V/cm	8×10^{-9}	1.4×10^{-2}	1.7
<u>Ge:Zn</u>			
T = 5.6 K E = 0.5 V/cm	2.5×10^{-8}	3.0×10^{-3}	1.2
T = 7.0 K E = 0.5 V/cm	1.5×10^{-8}	5.5×10^{-5}	0.9



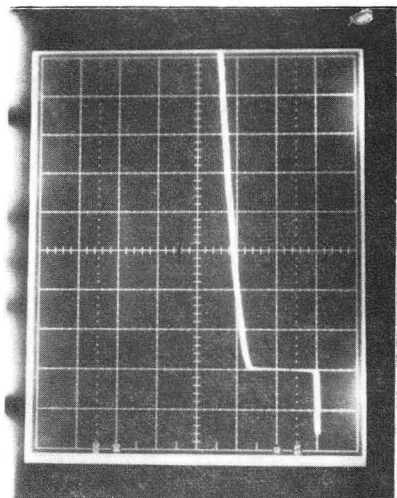
XBL 843-1141

Fig. 1.



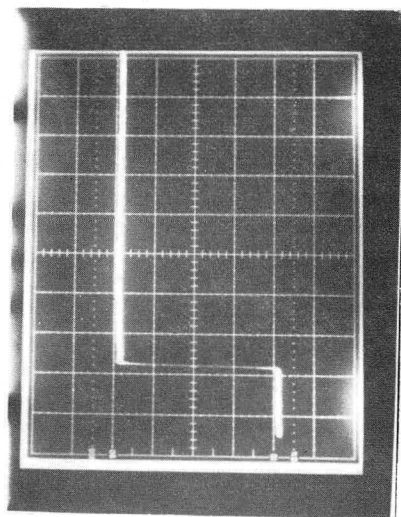
50 mV/DIV

0.5 SEC/DIV



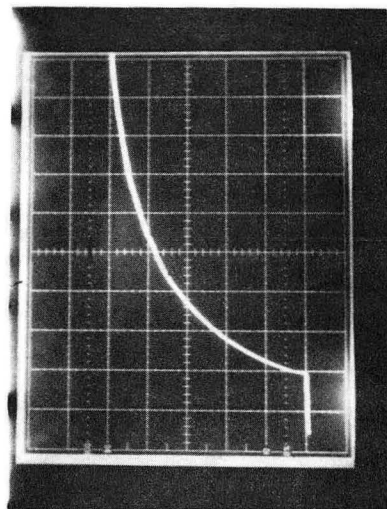
50 mV/DIV

0.5 SEC/DIV



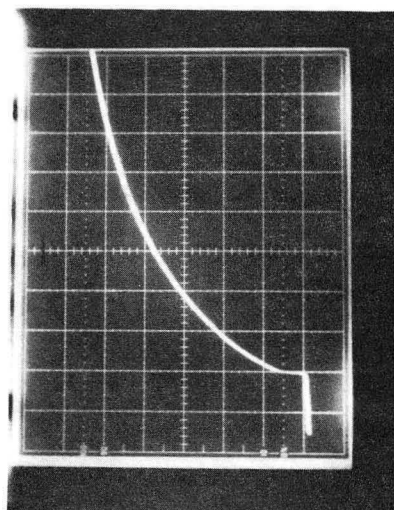
20 mV/DIV

0.5 SEC/DIV



0.2 V/DIV

0.5 SEC/DIV

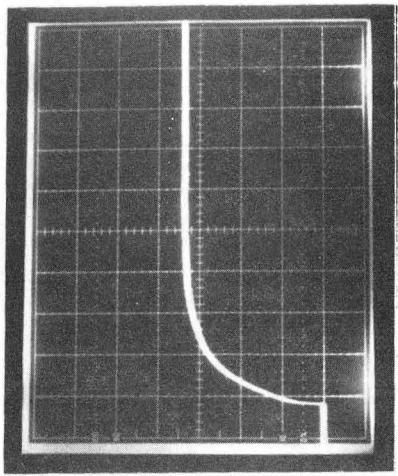


0.1 V/DIV

0.5 SEC/DIV

XBB 849-6802

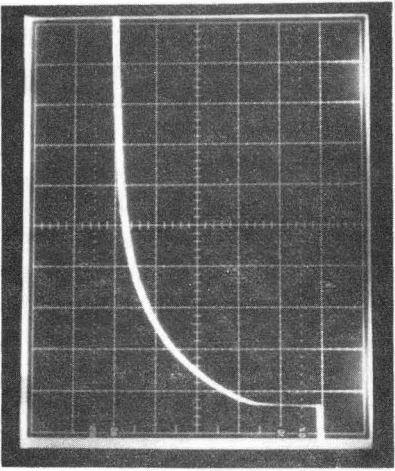
Fig. 2.



20 mV/DIV

(a)

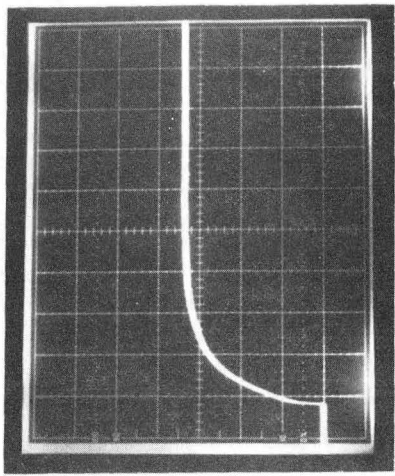
0.5 SEC/DIV



20 mV/DIV

(b)

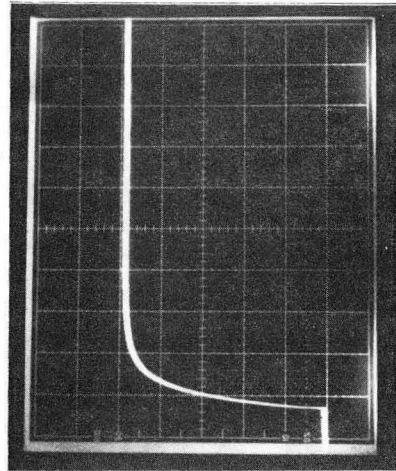
0.5 SEC/DIV



50 mV/DIV

(c)

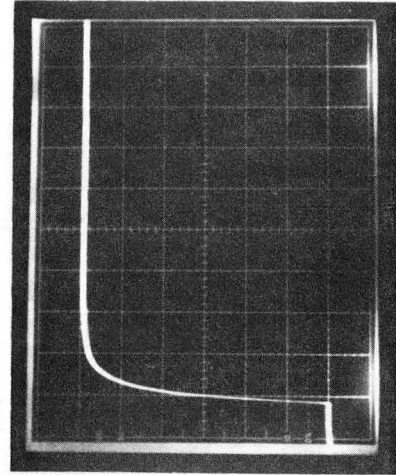
0.5 SEC/DIV



50 mV/DIV

(d)

0.5 SEC/DIV



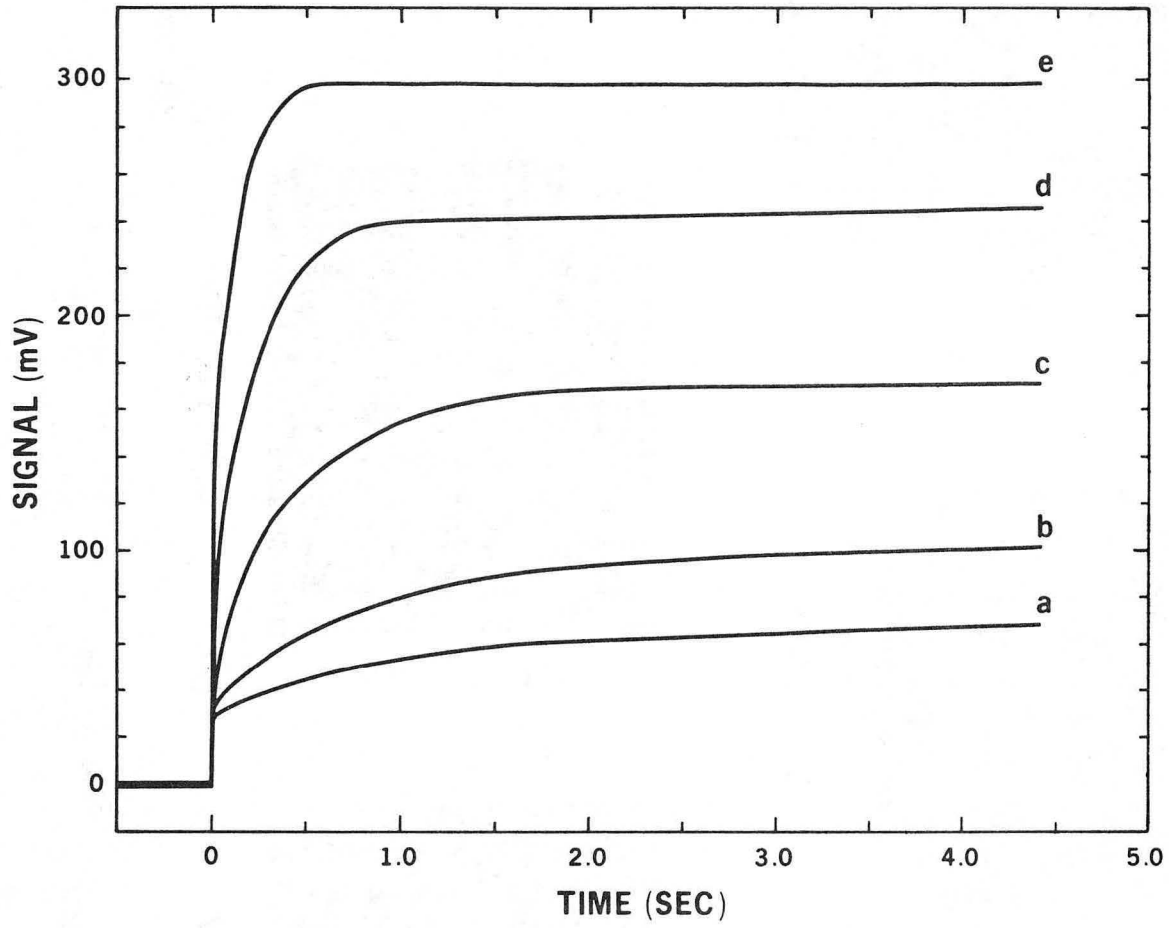
50 mV/DIV

(e)

0.5 SEC/DIV

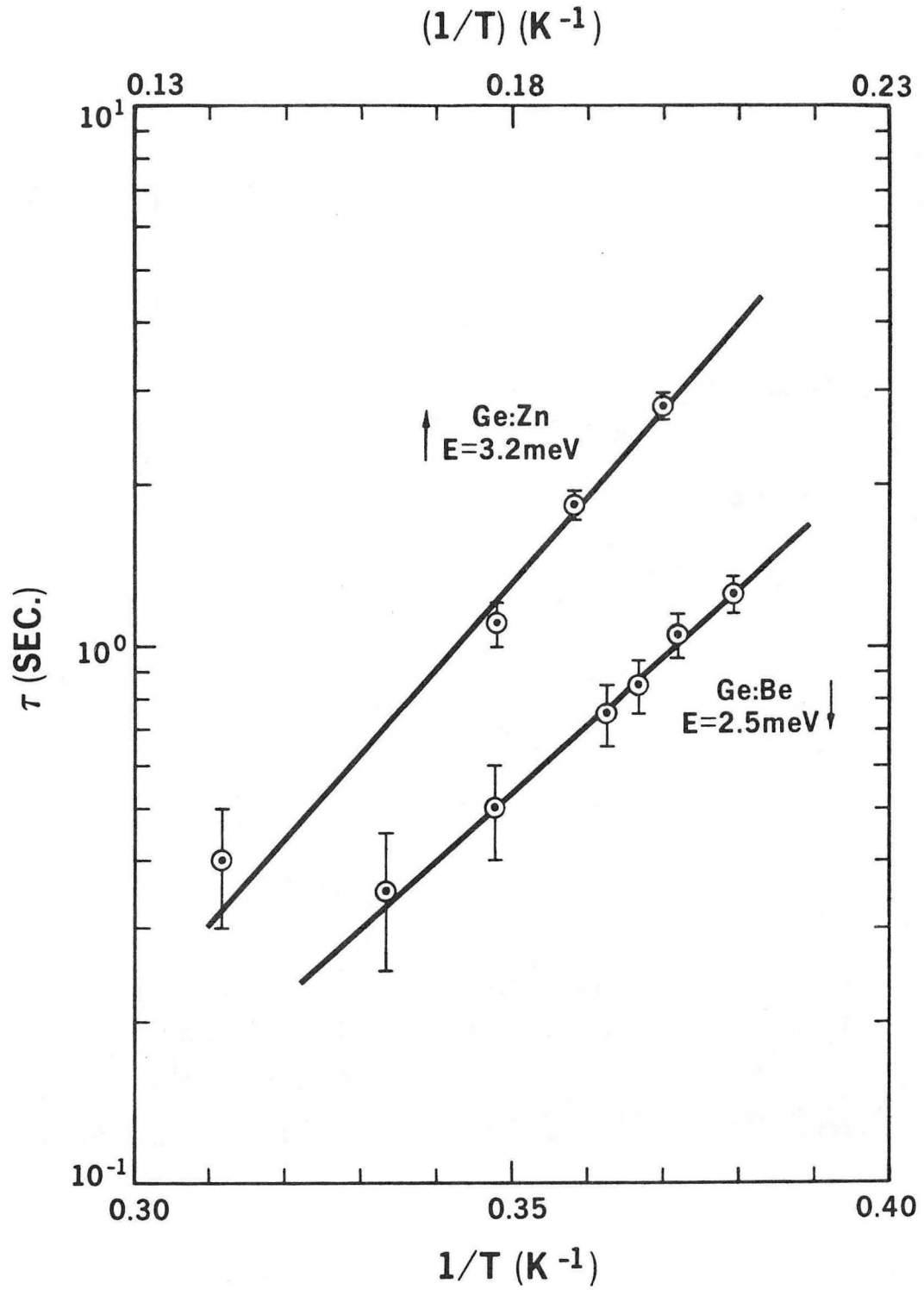
XBB 858-6089

Fig. 3.



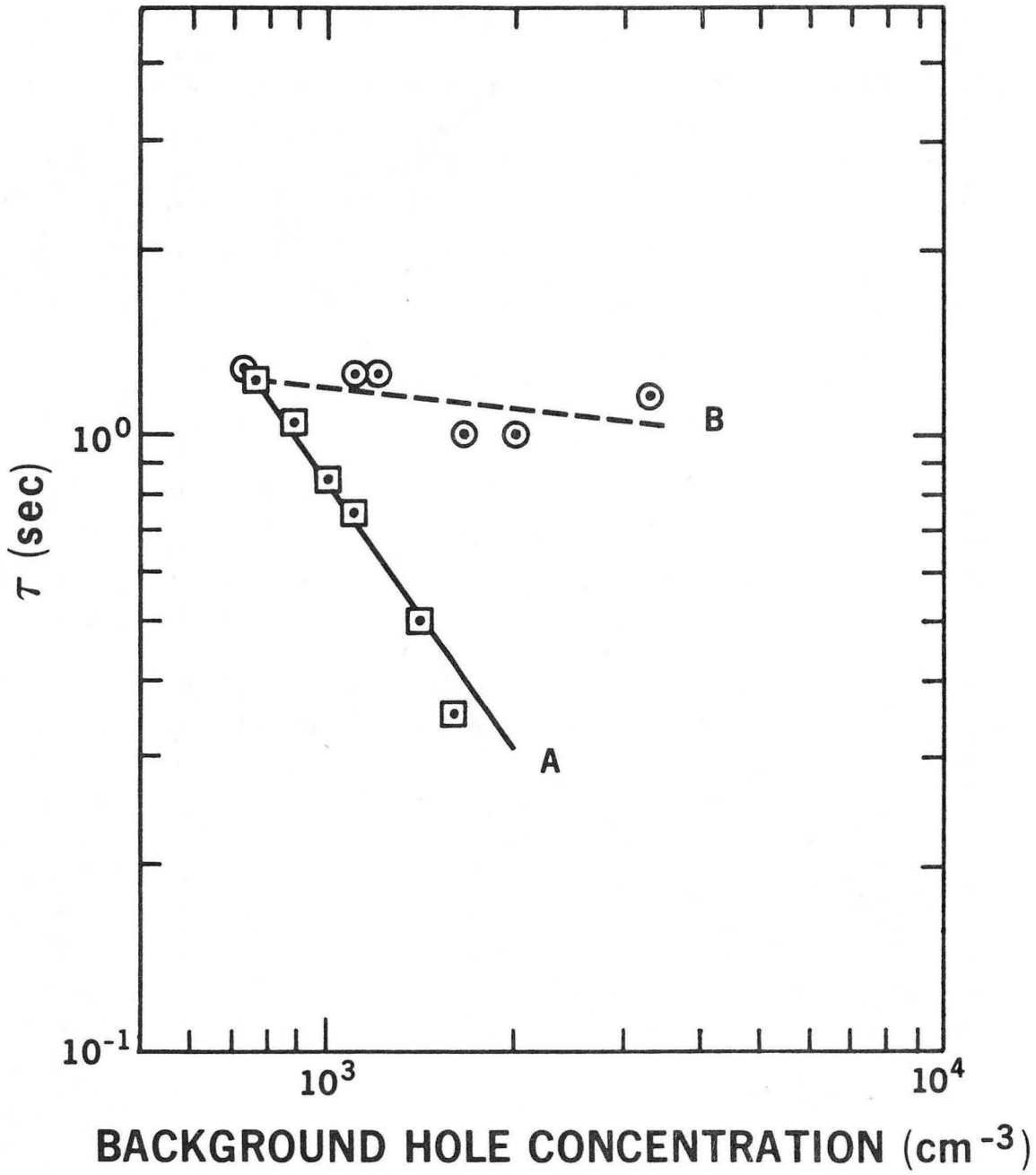
XBL 858 3766A

Fig. 4.



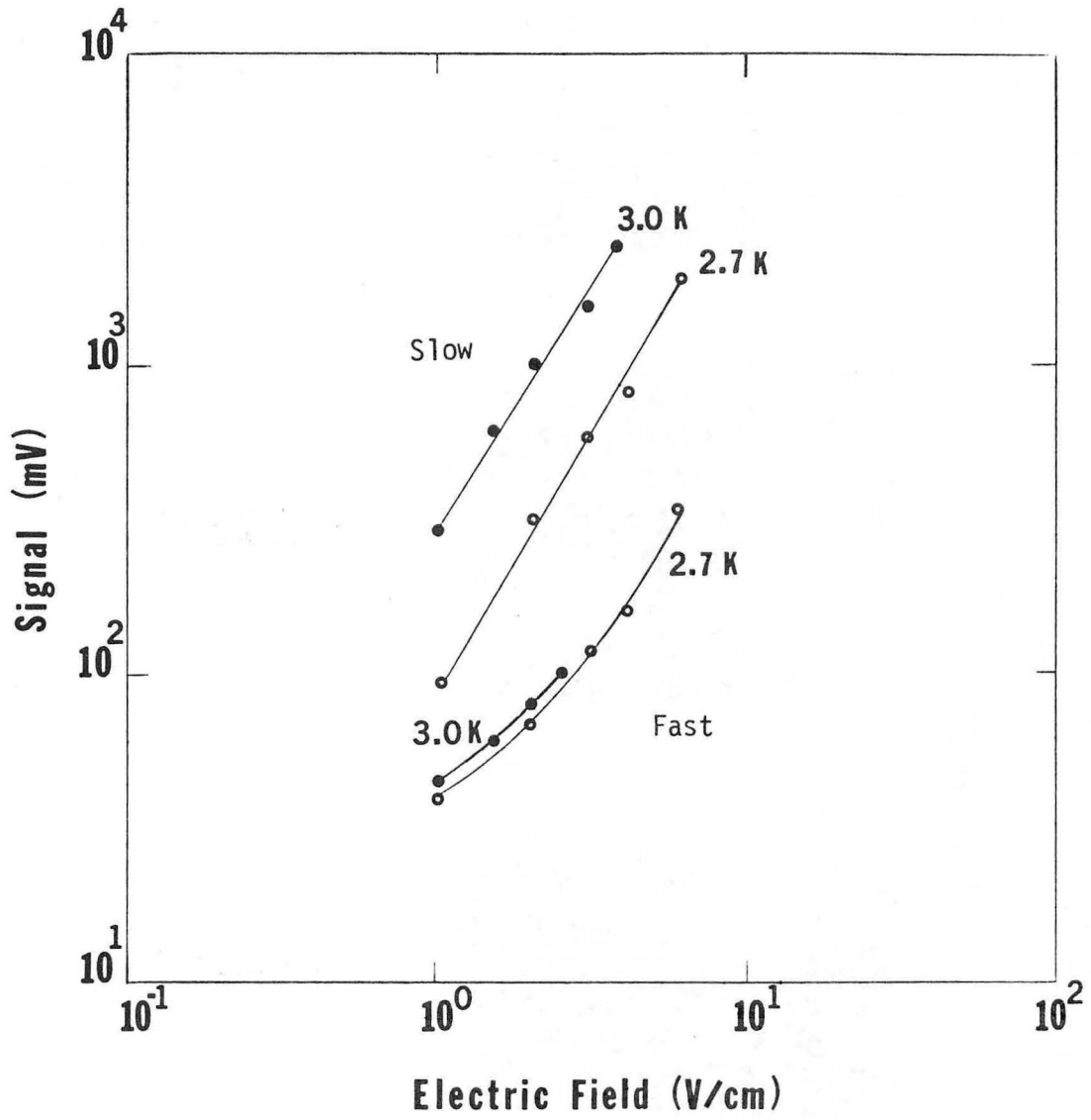
XBL 8510-4306

Fig. 5.



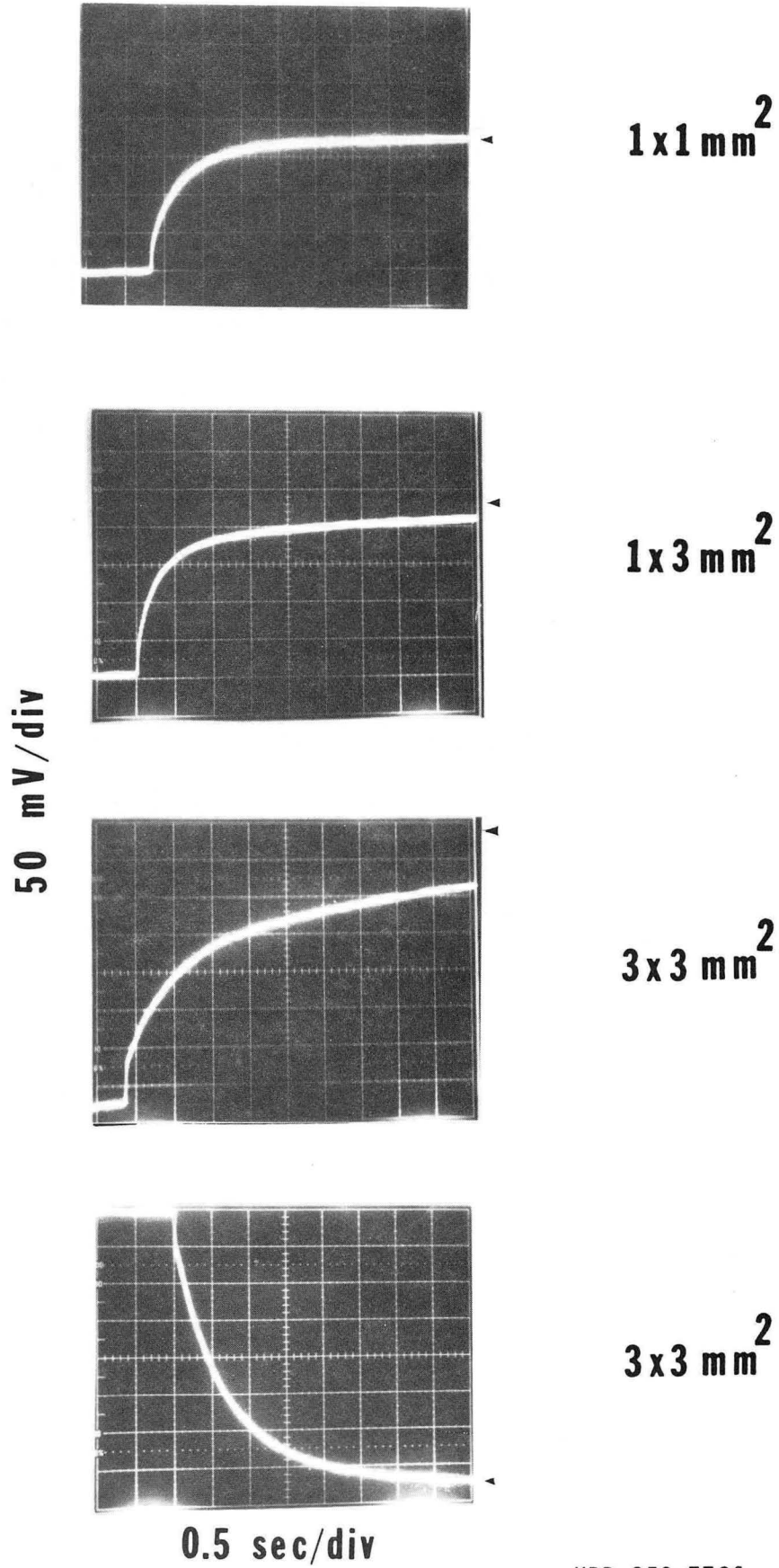
XBL 8510-4307

Fig. 6.



XBL 8510-4305

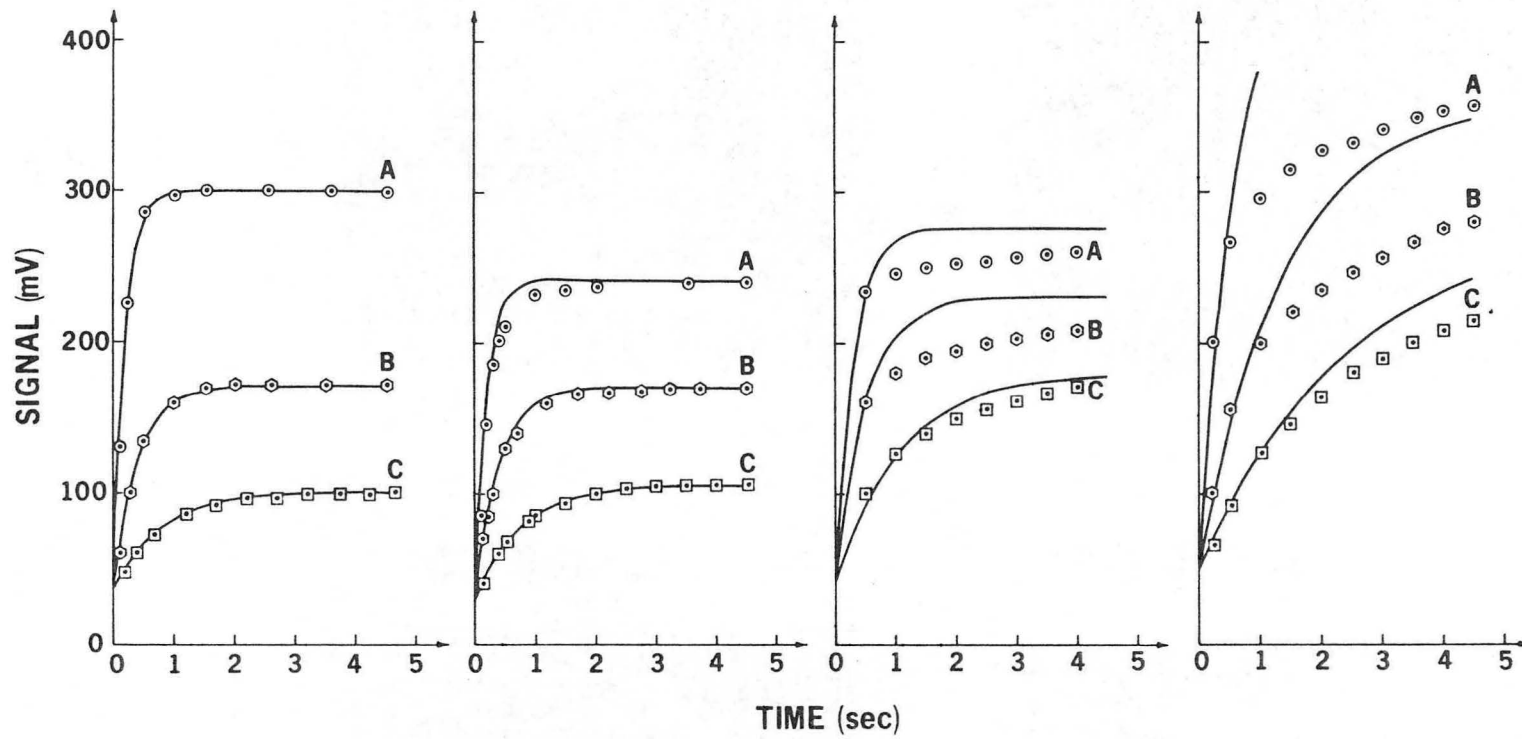
Fig. 7.



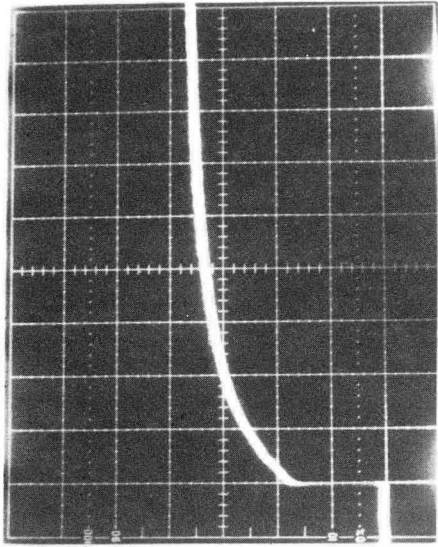
XBB 859-7736

Fig. 8.

Fig. 9.

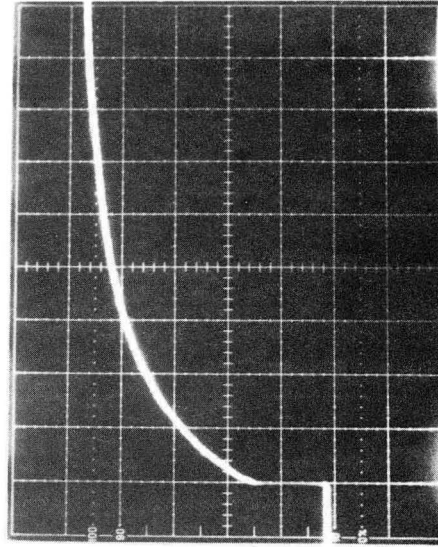


XBL 8510-4311



0.1 V/div

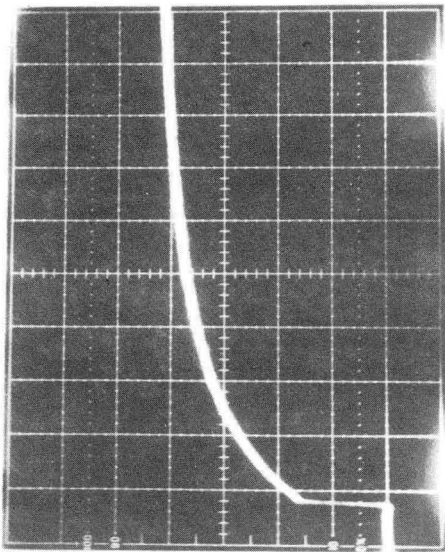
0.5 sec/div



0.1 V/div

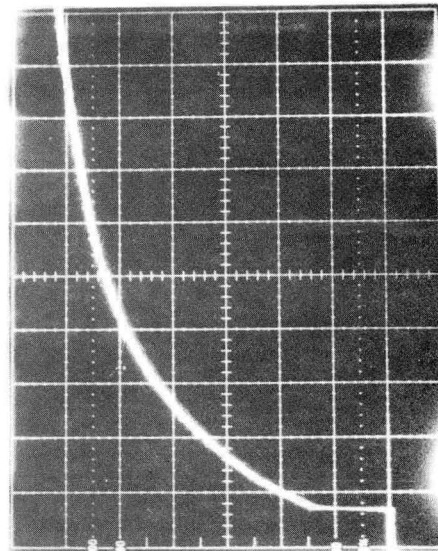
0.5 sec/div

XBB 859-7737



10 mV/div

0.5 sec/div



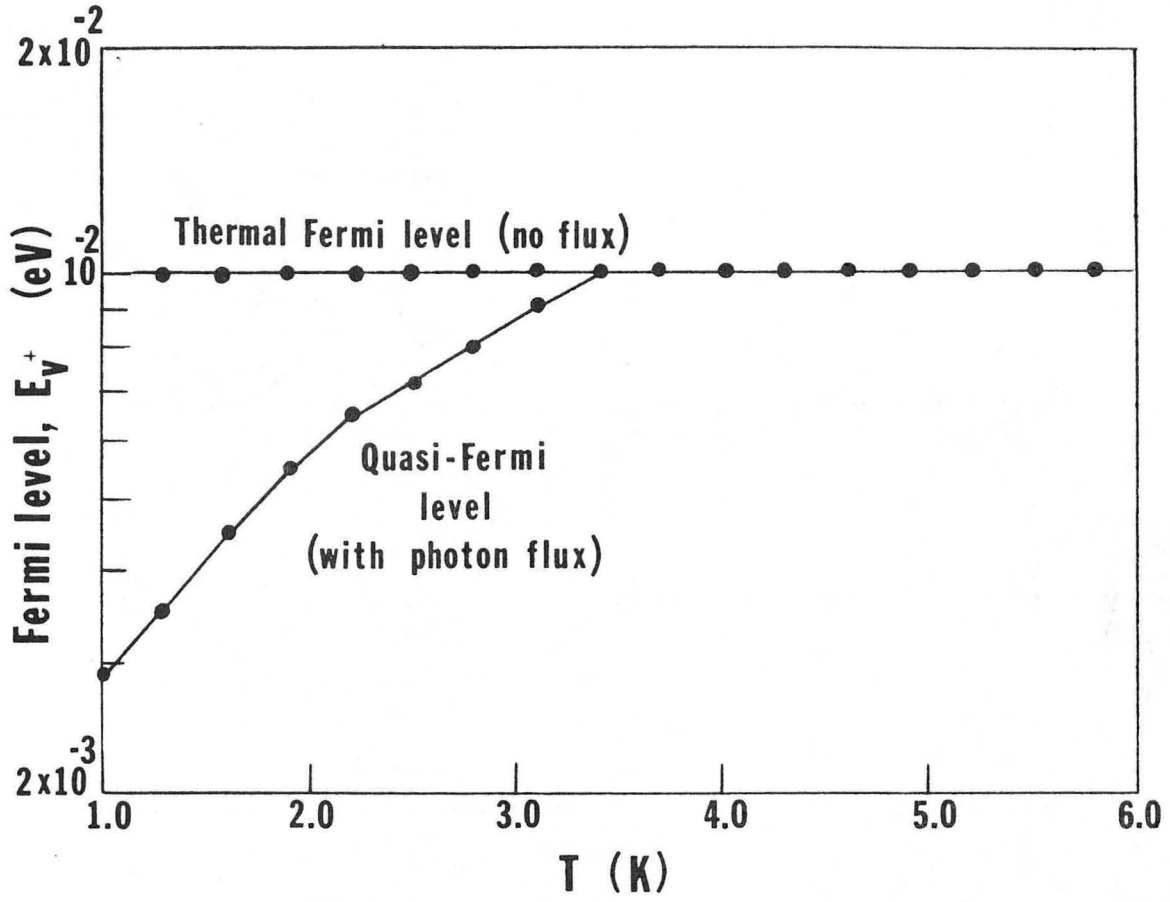
10 mV/div

0.5 sec/div

1 V/cm

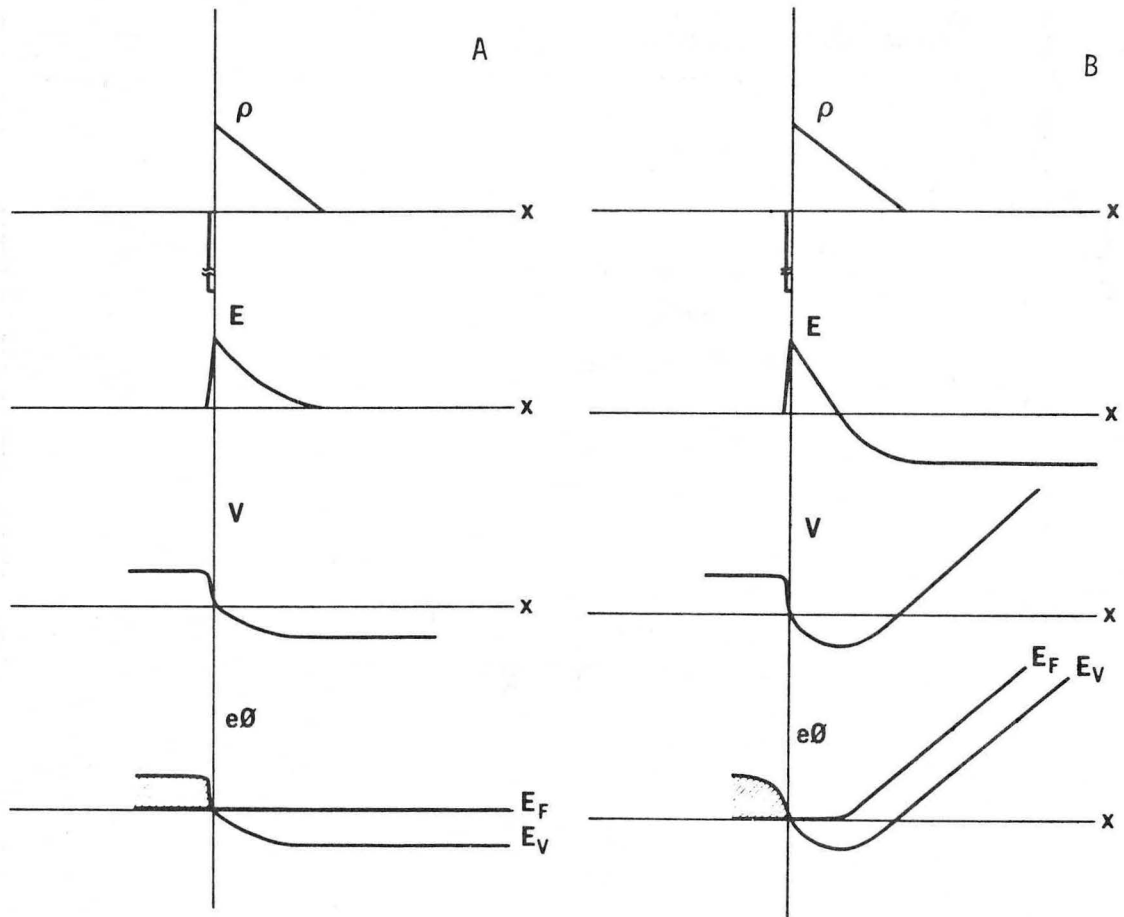
6 V/cm

Fig. 10.



XBL 8510-4200

Fig. 11.



XBL 8510-4310

XBL 8510-4309

Fig. 12.

This report was done with support from the Department of Energy. Any conclusions or opinions expressed in this report represent solely those of the author(s) and not necessarily those of The Regents of the University of California, the Lawrence Berkeley Laboratory or the Department of Energy.

Reference to a company or product name does not imply approval or recommendation of the product by the University of California or the U.S. Department of Energy to the exclusion of others that may be suitable.

*LAWRENCE BERKELEY LABORATORY
TECHNICAL INFORMATION DEPARTMENT
UNIVERSITY OF CALIFORNIA
BERKELEY, CALIFORNIA 94720*